SUPPLEMENTARY INFORMATION

Fluorescent 2D Metal-Organic Framework Nanosheets (MONs): Design, Synthesis and Sensing of Explosive Nitroaromatic Compounds (NACs)

Vijay Kumar Maka, Arindam Mukhopadhyay, Govardhan Savitha and Jarugu Narasimha Moorthy*

Department of Chemistry, Indian Institute of Technology, Kanpur 208016, INDIA

E-mail: moorthy@iitk.ac.in

CONTENTS

Table S1. Crystal data and refinement parameters for **In-TPA**.

Identification code	**In-TPA**	
Empirical formula	C78 H67 In42 N7 O16	
Formula weight	3176.04	
Temperature	100(2) K	
Wavelength	0.71073 Å	
Crystal system	Monoclinic	
Space group	C 2/c	
Unit cell dimensions	a = 23.254(3) Å	α= 90°
	b = 22.981(3) Å	β= 98.488(4)°
	c = 17.777(2) Å	γ = 90°
Volume	9396(2) $Å^3$	
Z	4	
Density (calculated)	1.123 mg/m^3	
Absorption coefficient	0.547 mm^{-1}	
F(000)	3240	
Crystal size	0.2 x 0.2 x 0.2 mm^3	
Theta range for data collection	2.117 to 25.090°	
Index ranges	$-27 \leq h \leq 27$, $-27 \leq k \leq 27$, $-21 \leq l \leq 21$	
Reflections collected	39236	
Independent reflections	8345 [R(int) = 0.1238]	
Completeness to theta = 25.090°	99.6 %	
Absorption correction	None	
Refinement method	Full-matrix least-squares on F^2	
Data / restraints / parameters	8345 / 0 / 421	
Goodness-of-fit on F^2	1.034	
Final R indices [I>2sigma(I)]	R_1 = 0.0883, wR_2 = 0.2638	
R indices (all data)	R_1 = 0.1509, wR_2 = 0.3074	
Largest diff. peak and hole	1.986 and -1.463 $eÅ^{-3}$	

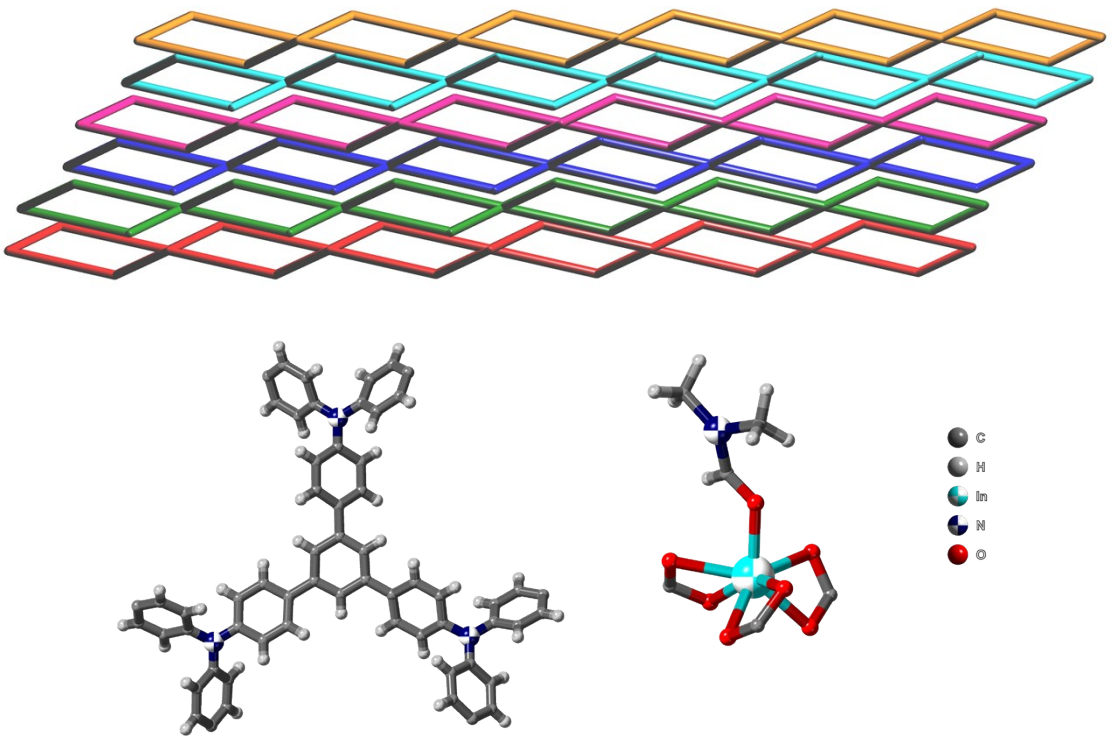

Fig. S1 Simplified topological network of **In-TPA** and building units considered for nodes. For topological analysis of **In-TPA,** the linker **TPA** without carboxylates was considered as one node and Indium-tricarboxylate complex including DMF was considered as the second node.

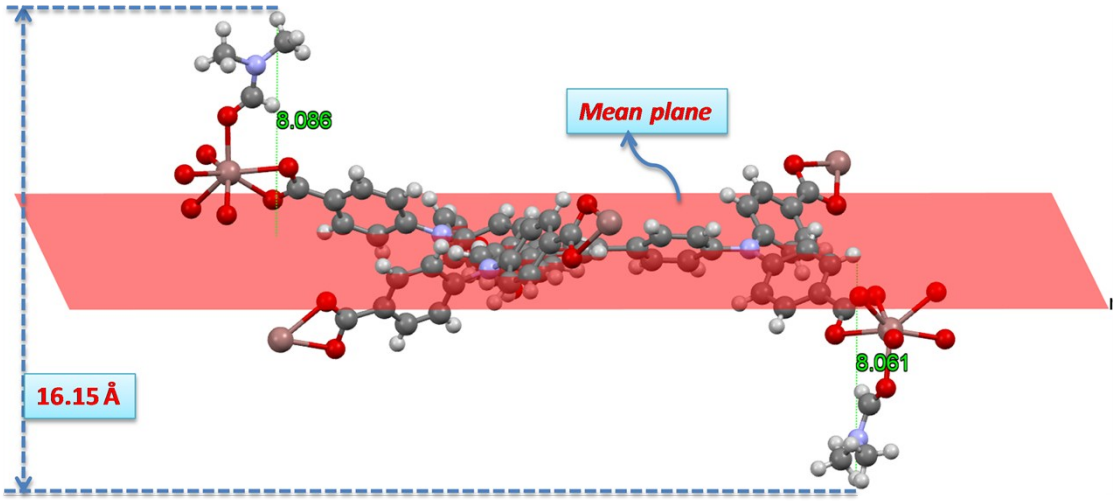

Fig. S2 Crystal structure of **In-TPA** showing the thickness of a single layer. Notice that the thickness of a single layer is ca. 1.61 nm.

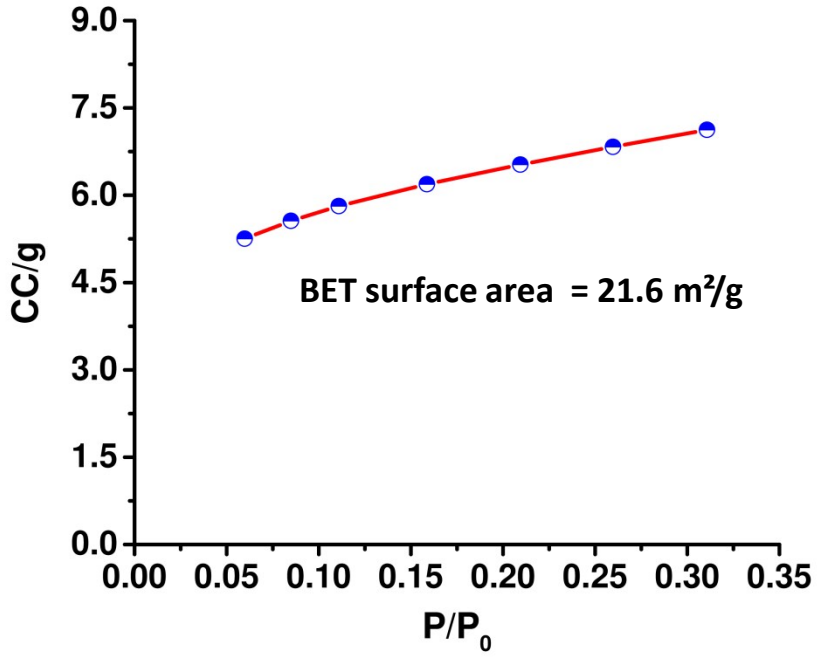

Fig. S3 BET surface area analysis of **In-TPA**.

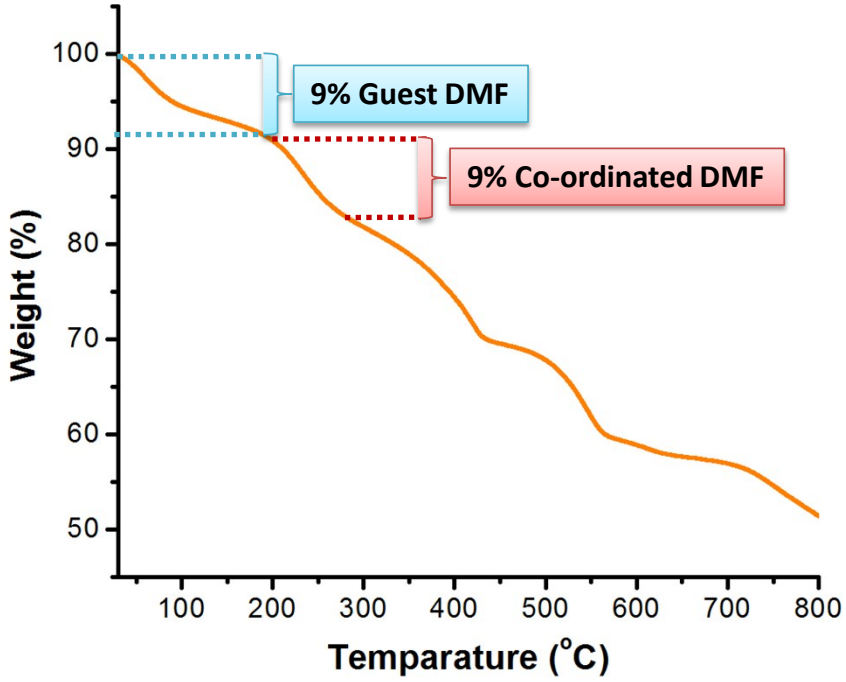

Fig. S4 TGA profile of pristine **In-TPA**.

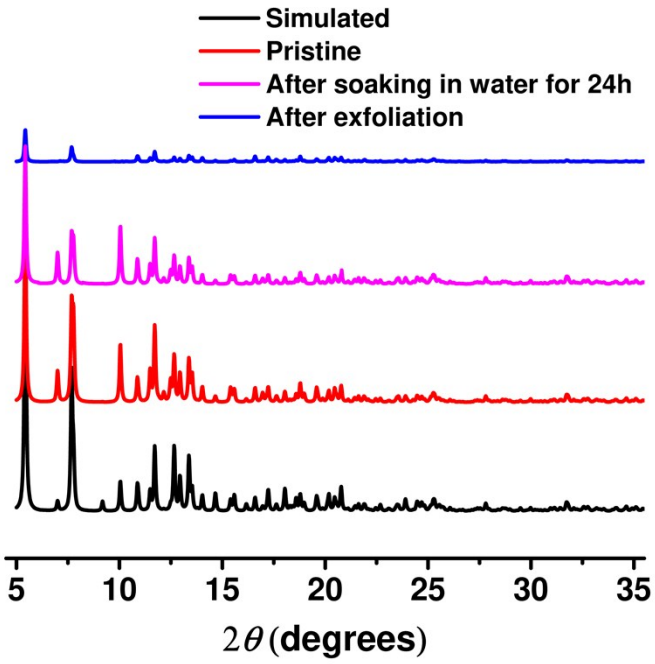

Fig. S5 PXRD profiles of **In-TPA** simulated, pristine bulk material, after soaking in water for 24 h and after exfoliation.

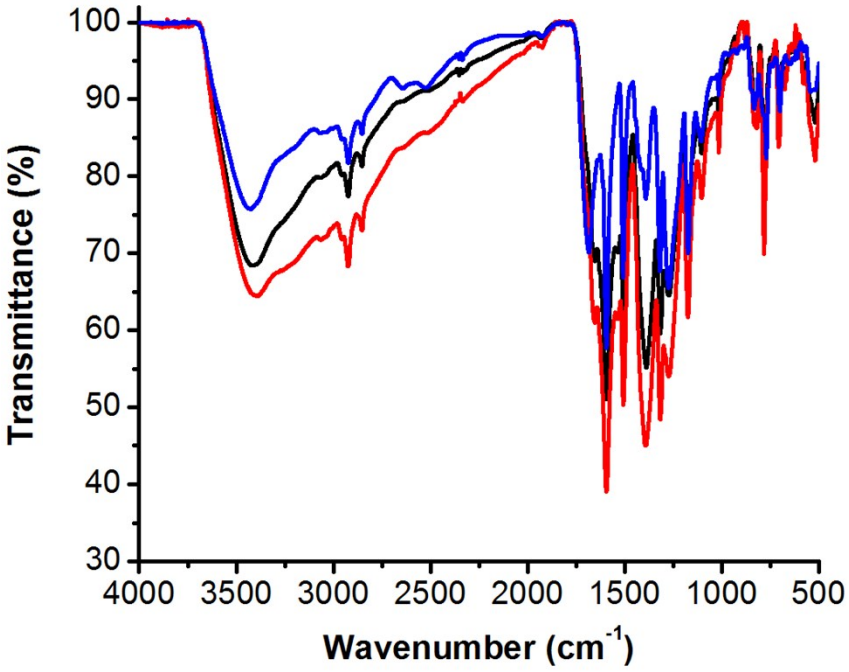

Fig. S6 IR (KBr) spectra of **H_6TPA** (blue line), **In-TPA** pristine (black line) and after (red line) exfoliation.

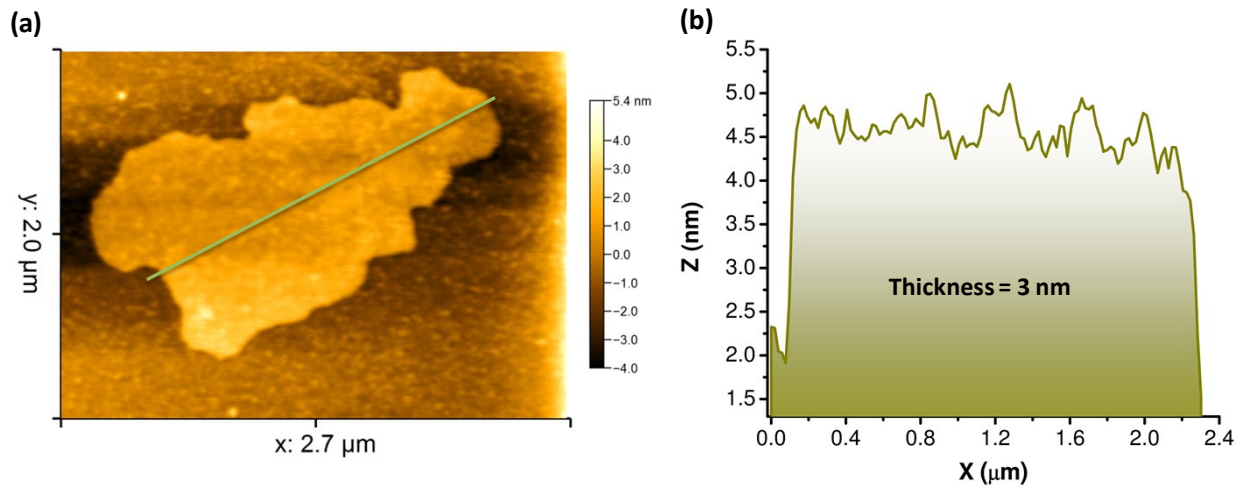

Fig. S7 a) AFM image and (b) corresponding height profile diagram for the 2D nanosheet of **In-TPA**.

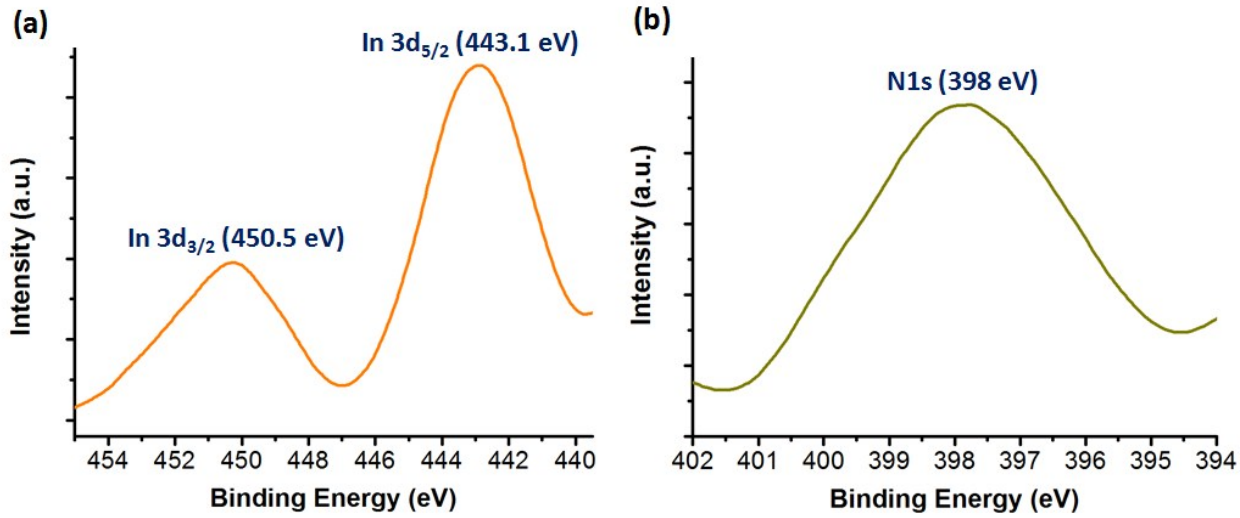

Fig. S8 XPS analysis of the exfoliated 2D nanosheets of **In-TPA** deposited on silicon wafers.

Dynamic Light Scattering (DLS) Experiment. For DLS analysis of the 2D MONs of **In-TPA**, 2.0 mg of the crystals of pristine **In-TPA** in ethanol (10 mL) were subjected to sonication for 60 min, and the particle size distribution of the resultant suspension was analyzed immediately. The DLS experiments were carried out using a 'Malvern Zetasizer' particle size analyzer at 298 K. As shown below, the mean particle size of the material was found to be 310 nm.

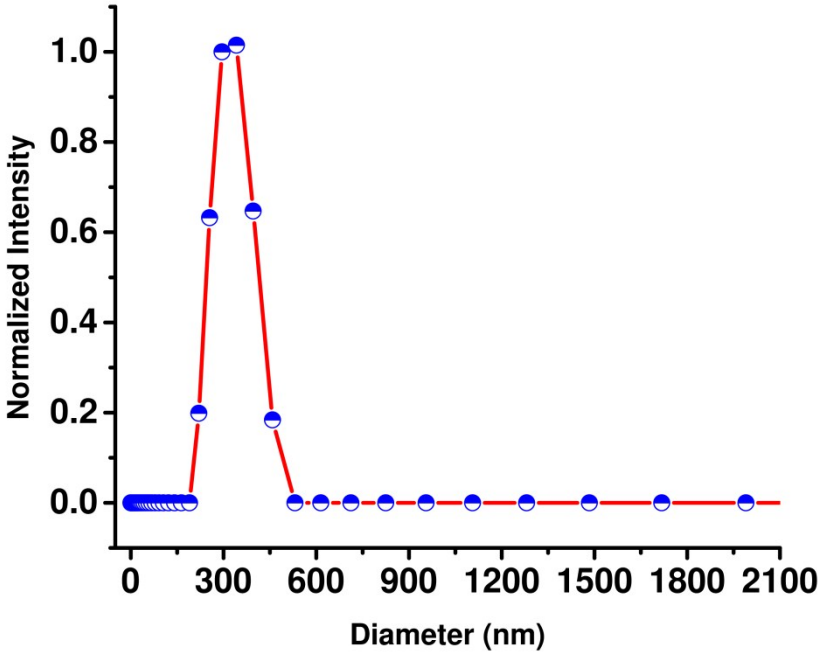

Fig. S9 Plot of particle size distribution for 2D MONs of **In-TPA** with respect to scattering normalized intensity obtained by DLS analysis after 60 min of ultrasonication in ethanol.

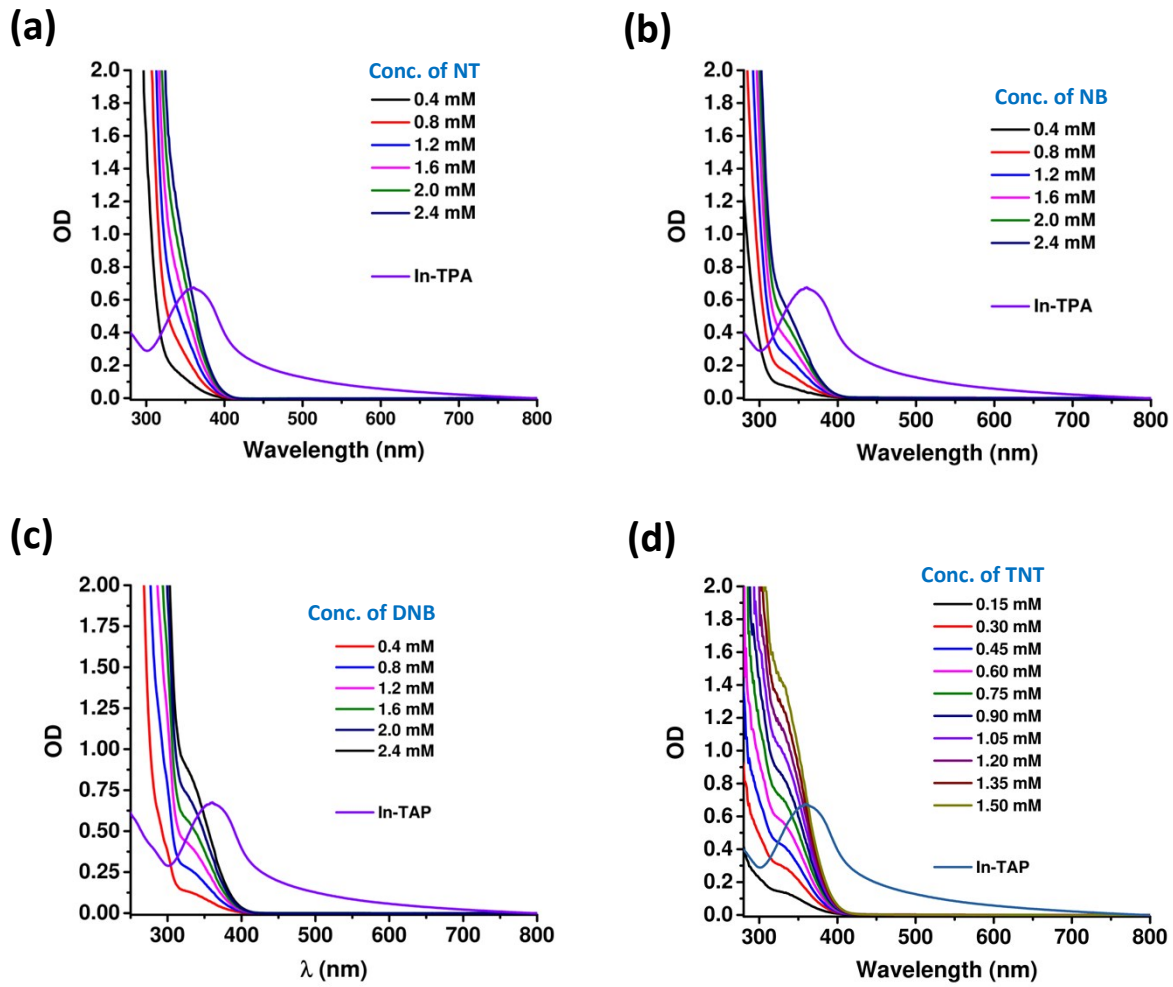

Fig. S10 UV-vis absorption spectra of NACs at different concentrations and that of **In-TPA** in ethanol.

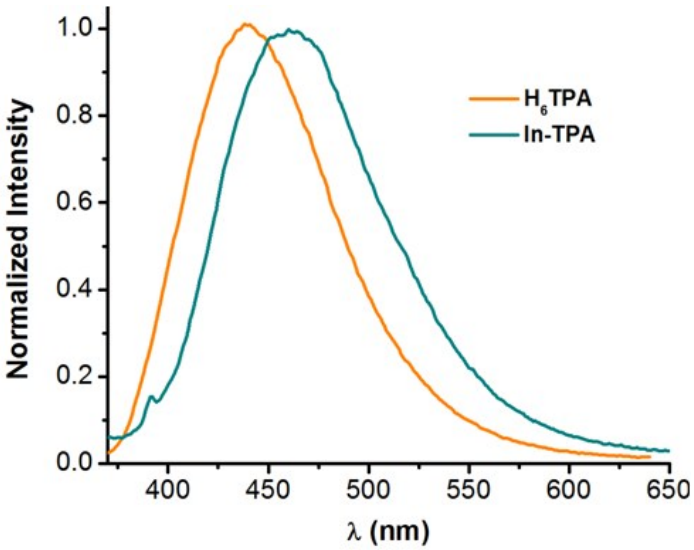

Fig. S11 Fluorescence emission spectra of **H_6TPA** (orange line) and **In-TPA** (cyan line) for excitation at 350 nm in ethanol.

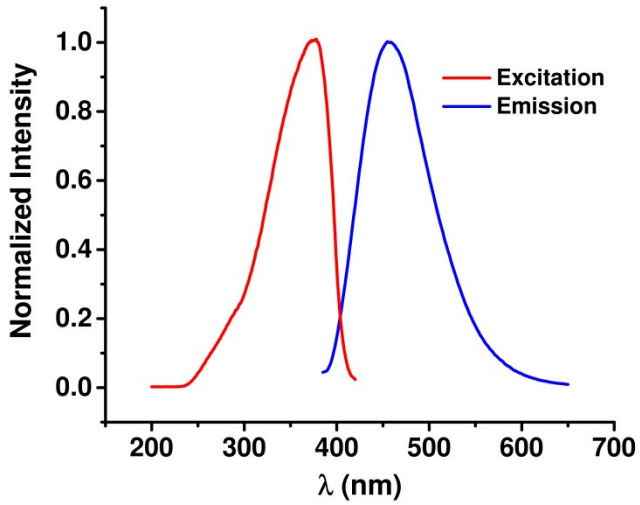

Fig. S12 Fluorescence excitation (λ_{emi} = 460 nm) and emission (λ_{ex} = 370 nm) spectra of **In-TPA** in ethanol.

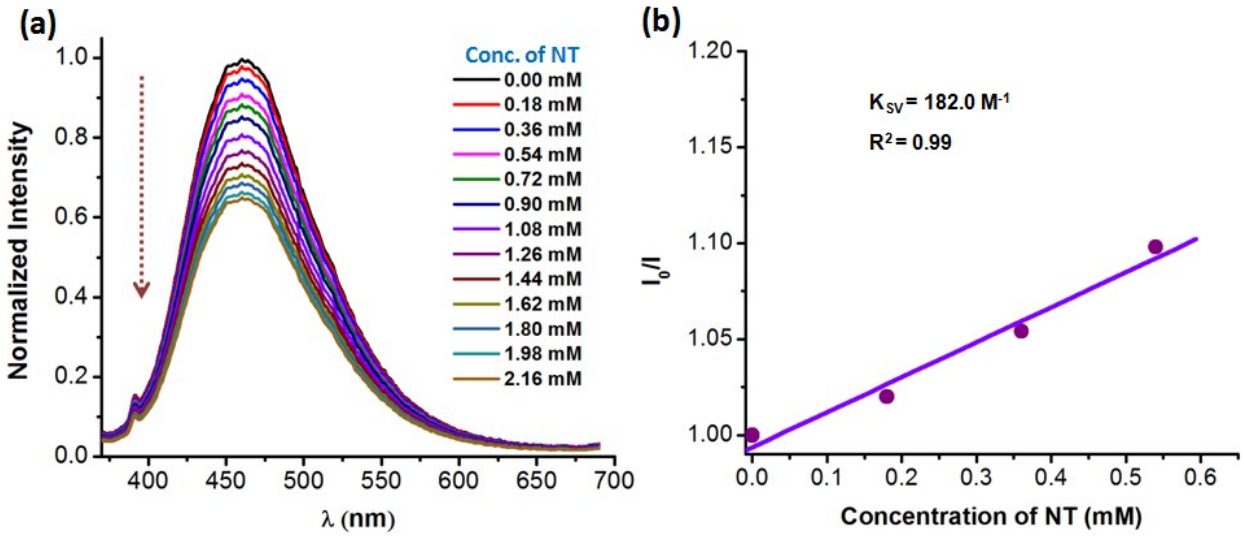

Fig. S13 (a) Quenching of fluorescence intensity of **In-TPA** with increasing concentration of NT in ethanol (λ_{ex} = 350 nm). (b) Determination of the Stern-Volmer quenching constant.

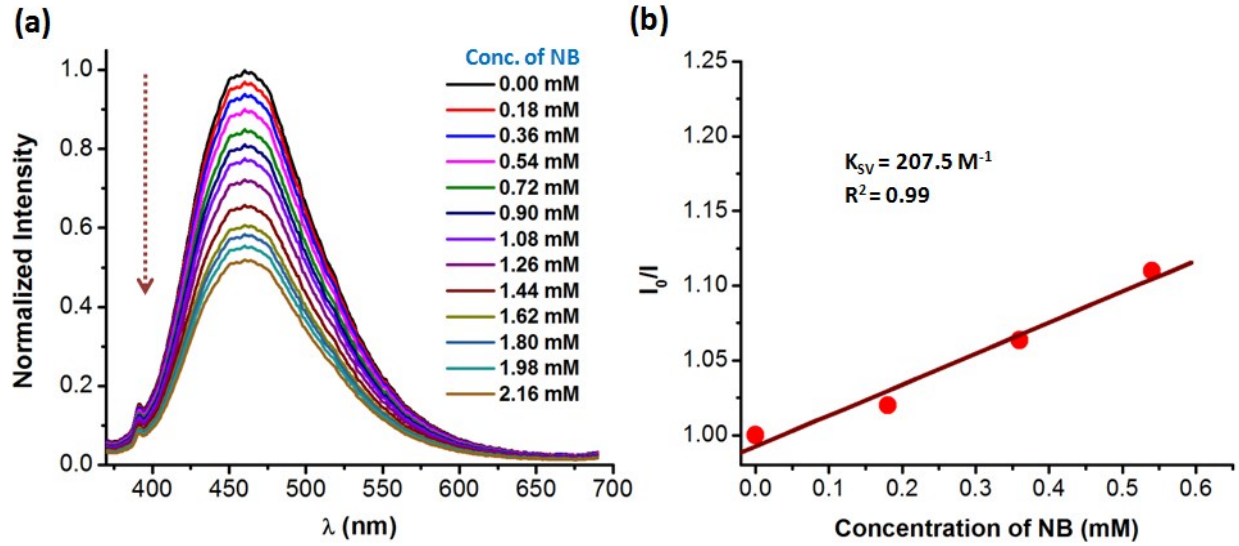

Fig. S14 (a) Quenching of fluorescence intensity of **In-TPA** with increasing concentration of NB in ethanol (λ_{ex} = 350 nm). (b) Determination of the Stern-Volmer quenching constant.

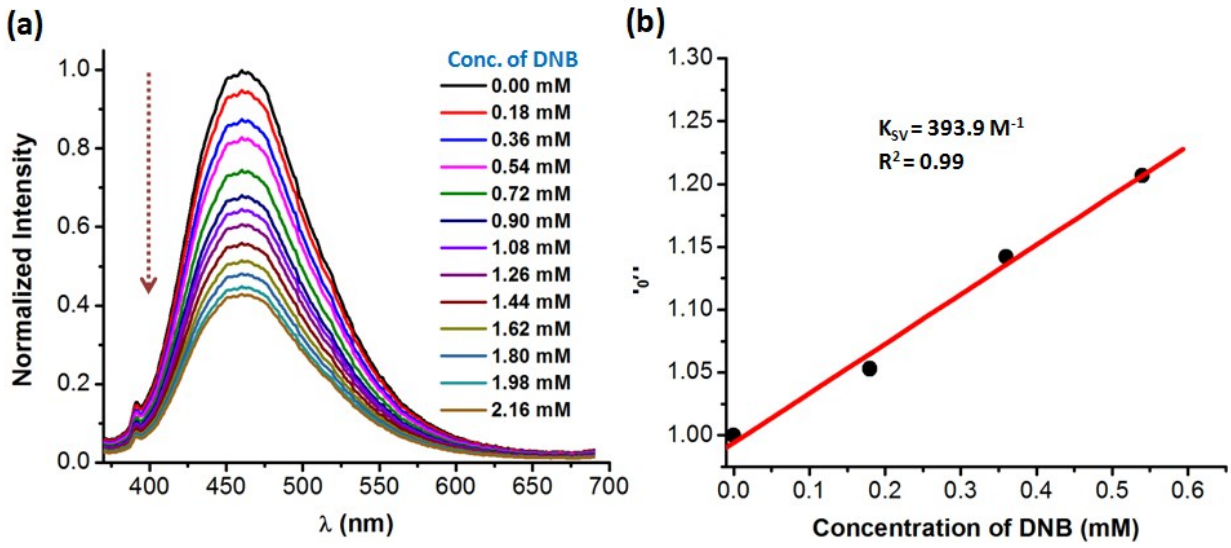

Fig. S15 (a) Quenching of fluorescence intensity of **In-TPA** with increasing concentration of DNB in ethanol (λ_{ex} = 350 nm). (b) Determination of the Stern-Volmer quenching constant.

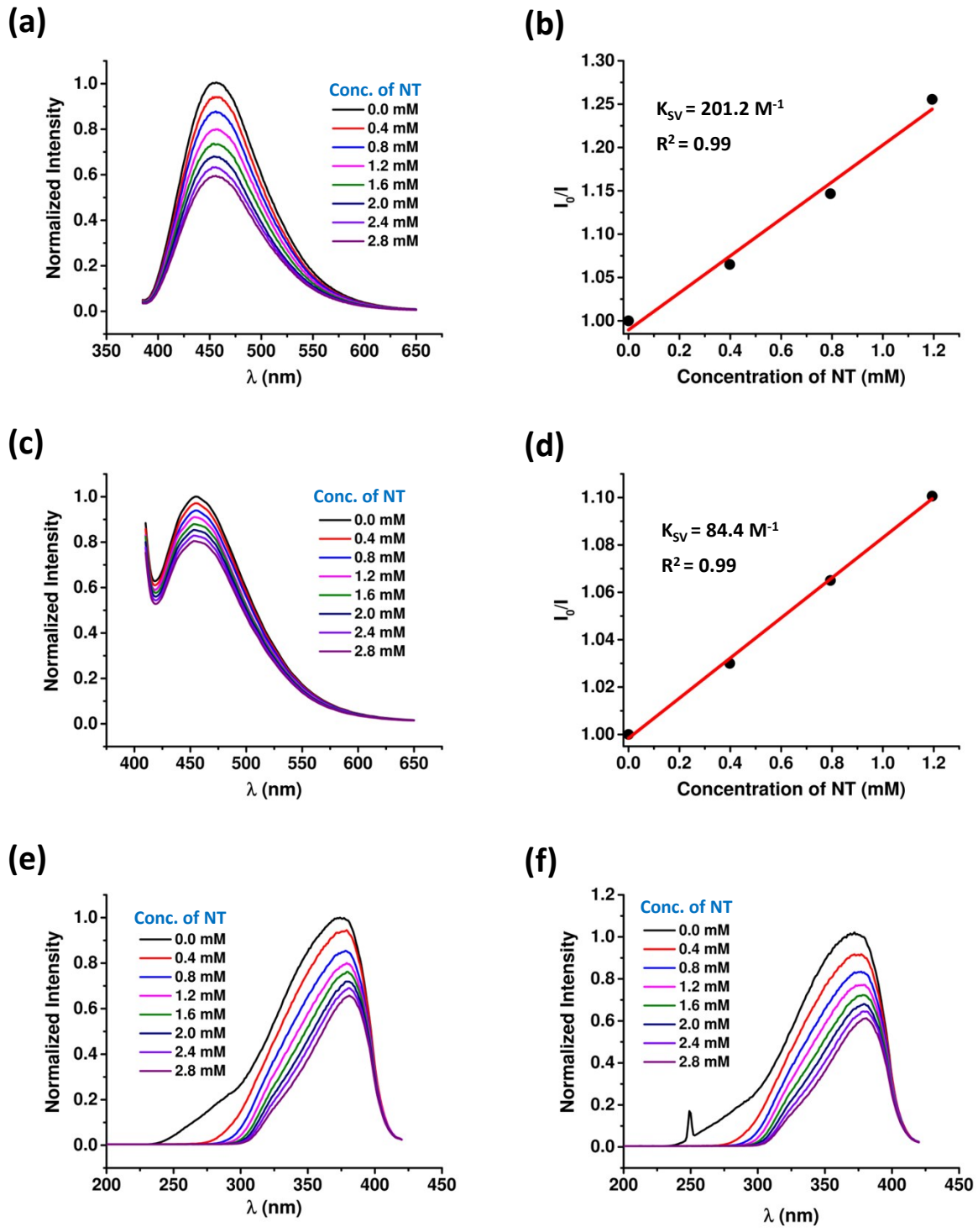

Fig. S16 Quenching of fluorescence of **In-TPA** with increasing concentration of NT in ethanol for excitation at 370 nm (a) and at 400 nm (c). Determination of Stern-Volmer quenching constants for excitation at 370 nm (b) and 400 nm (d). Excitation spectra of **In-TPA** with increasing concentration of NT in ethanol recorded with λ_{emi} = 460 nm (e) and λ_{emi} = 500 nm (f).

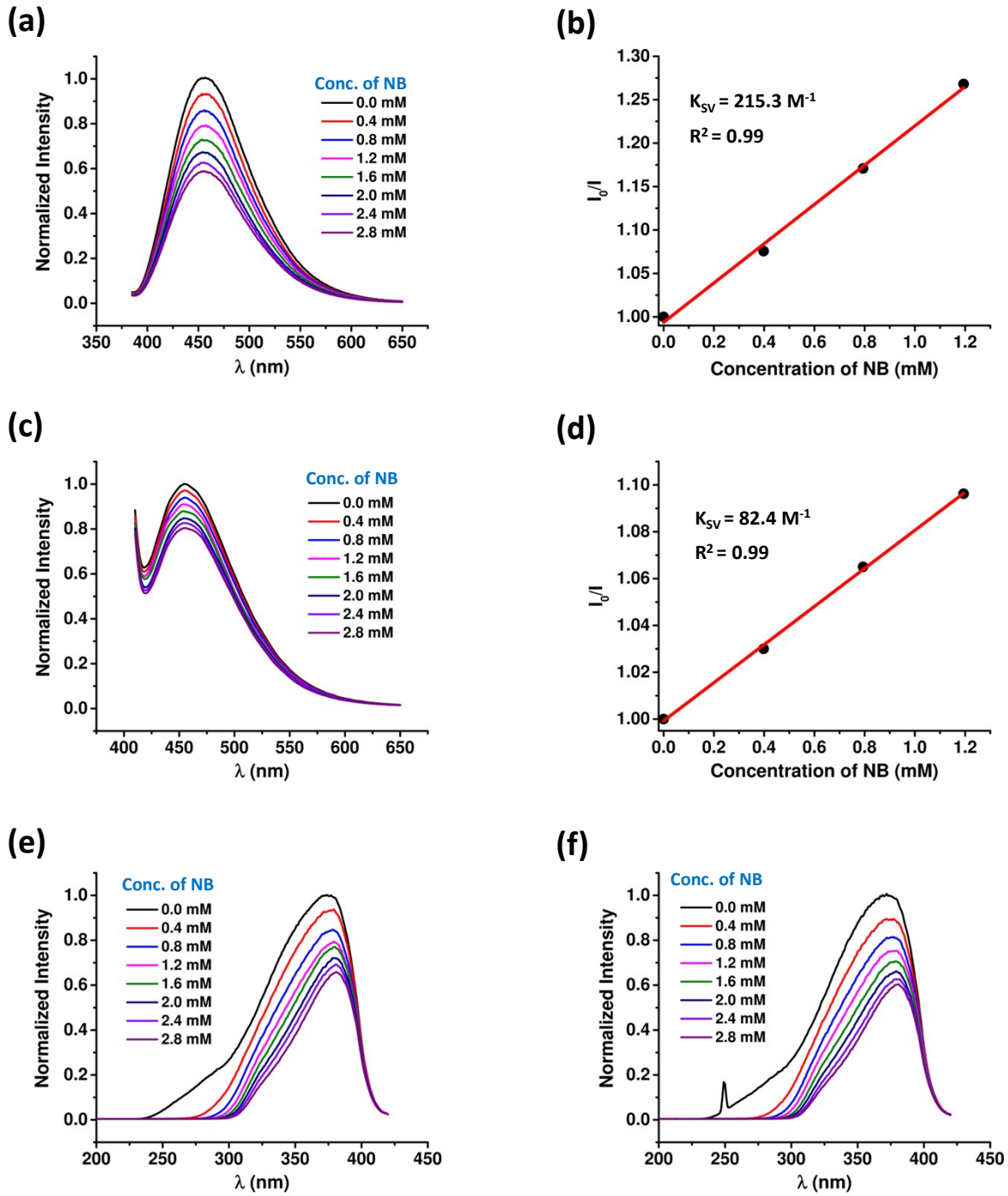

Fig. S17 Quenching of fluorescence of **In-TPA** with increasing concentration of NB in ethanol for excitation at 370 nm (a) and at 400 nm (c). Determination of Stern-Volmer quenching constants for excitation at 370 nm (b) and 400 nm (d). Excitation spectra of **In-TPA** with increasing concentration of NB in ethanol recorded with λ_{emi} = 460 nm (e) and λ_{emi} = 500 nm (f).

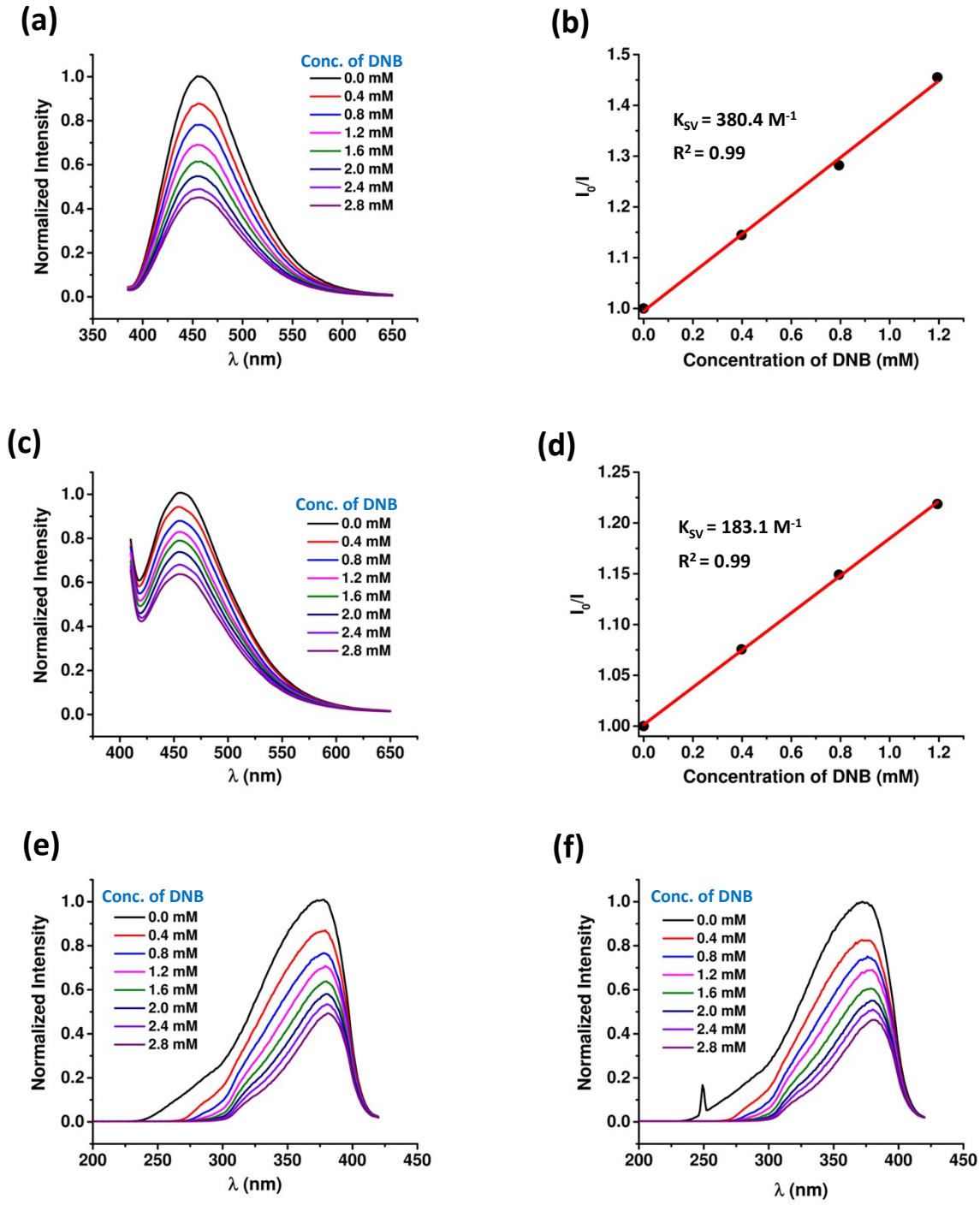

Fig. S18 Quenching of fluorescence of **In-TPA** with increasing concentration of DNB in ethanol for excitation at 370 nm (a) and at 400 nm (c). Determination of Stern-Volmer quenching constants for excitation at 370 nm (b) and 400 nm (d). Excitation spectra of **In-TPA** with increasing concentration of DNB in ethanol recorded with λ_{emi} = 460 nm (e) and λ_{emi} = 500 nm (f).

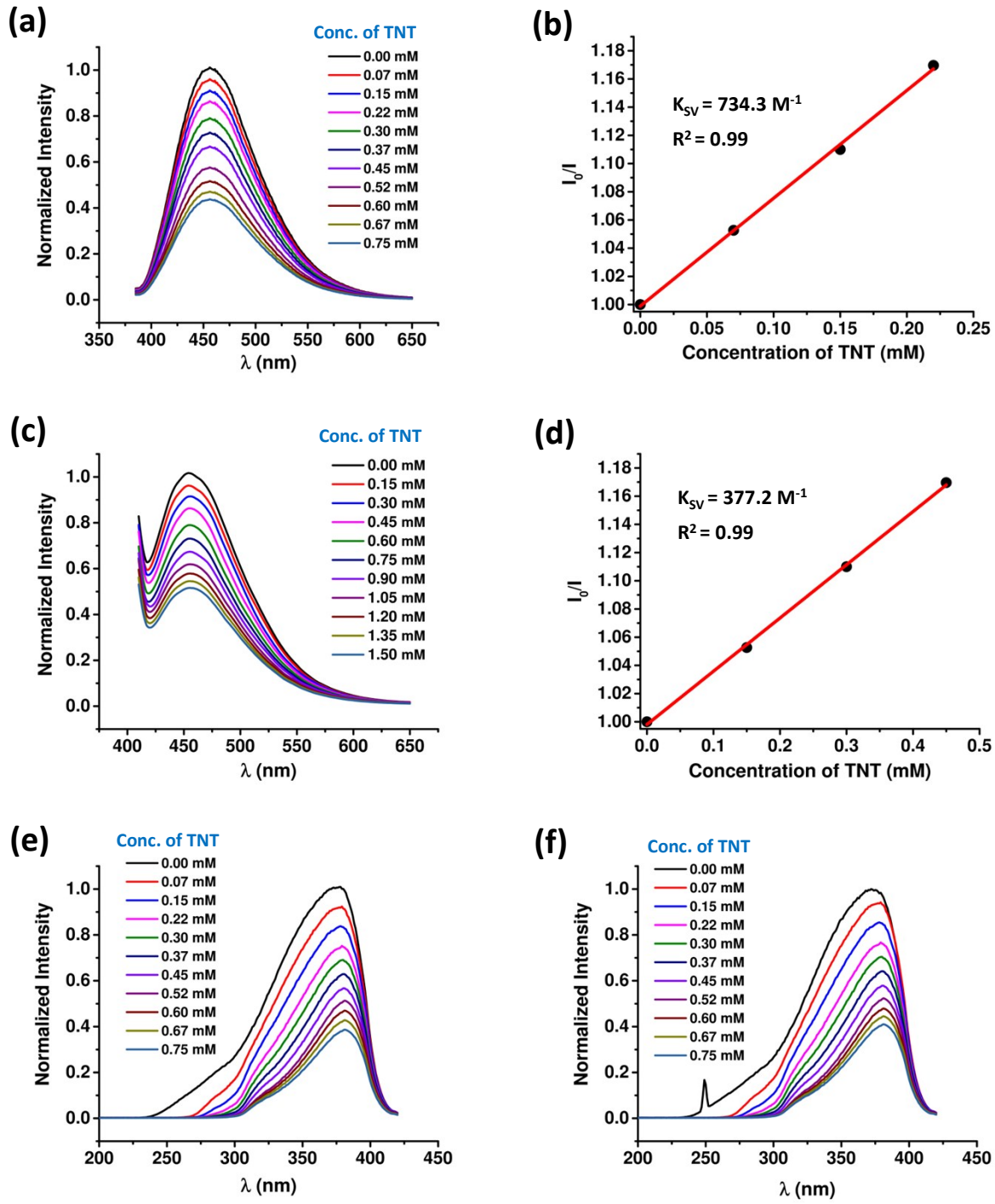

Fig. S19 Quenching of fluorescence of **In-TPA** with increasing concentration of TNT in ethanol for excitation at 370 nm (a) and at 400 nm (c). Determination of Stern-Volmer quenching constants for excitation at 370 nm (b) and 400 nm (d). Excitation spectra of **In-TPA** with increasing concentration of TNT in ethanol recorded with λ_{emi} = 460 nm (e) and λ_{emi} = 500 nm (f).

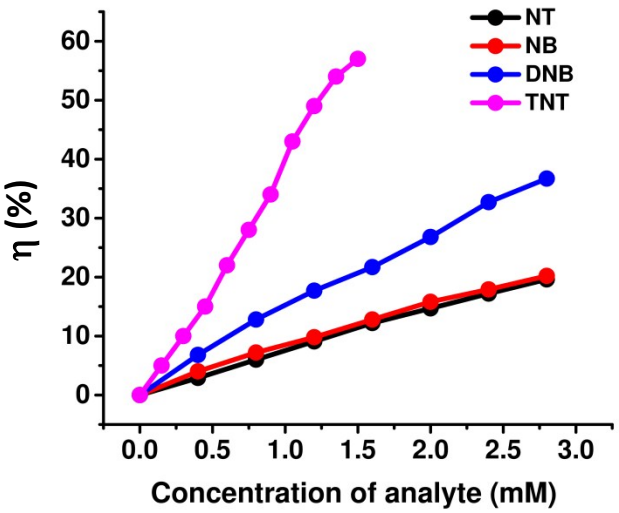

Fig. S20 Plot of fluorescence quenching efficiency (η%) versus concentration for each of the NACs for λ_{ex} of **In-TPA** at 400 nm.

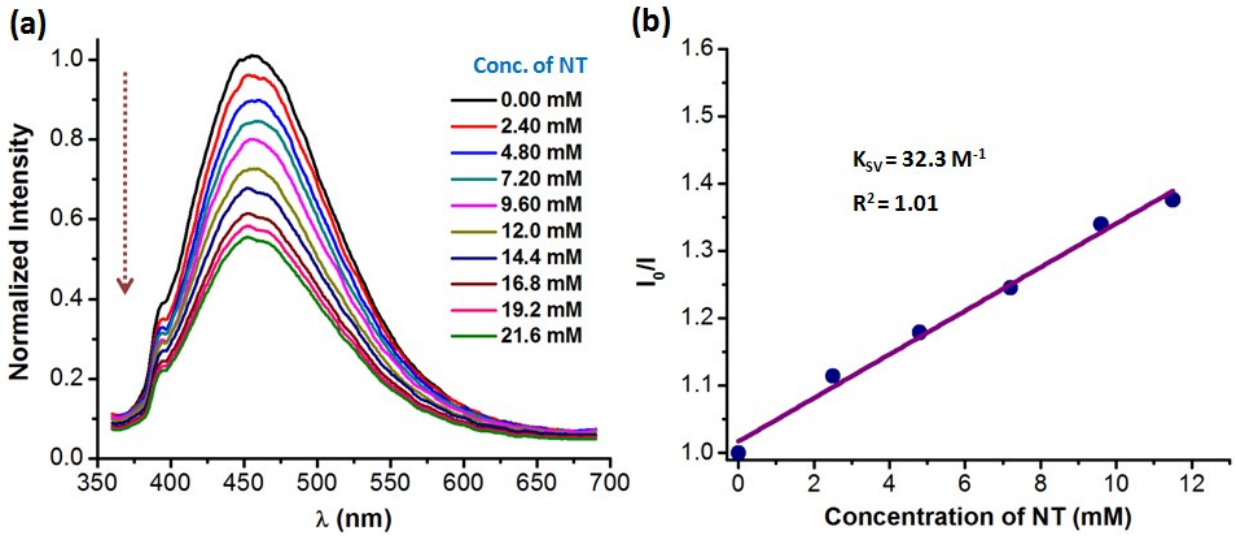

Fig. S21 (a) Quenching of fluorescence intensity of **H_6TPA** with increasing concentration of NT in ethanol (λ_{ex} = 350 nm). (b) Determination of the Stern-Volmer quenching constant.

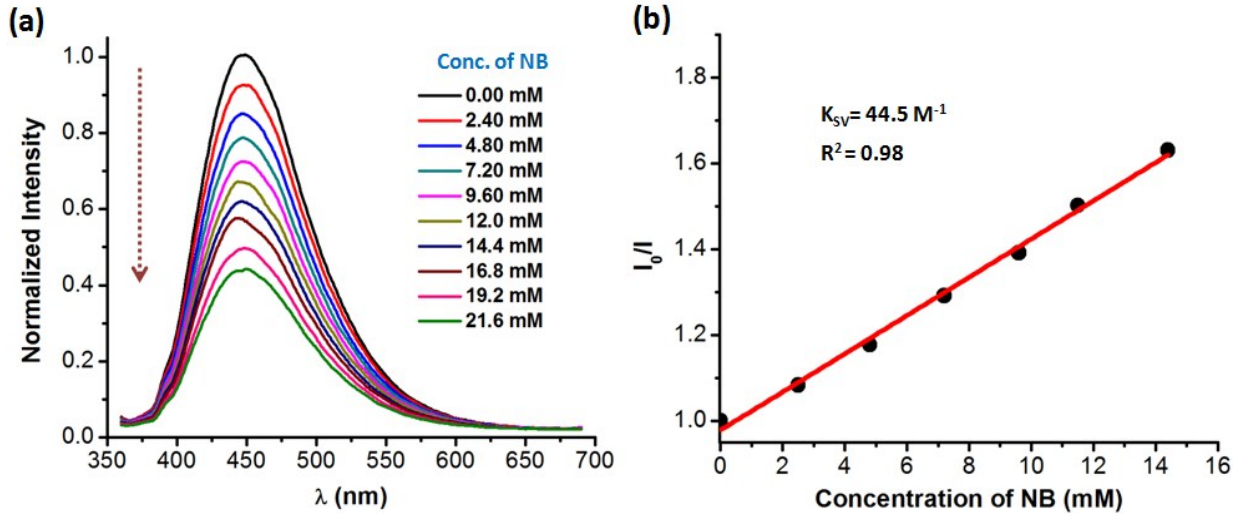

Fig. S22 (a) Quenching of fluorescence intensity of **H_6TPA** with increasing concentration of NB in ethanol (λ_{ex} = 350 nm). (b) Determination of the Stern-Volmer quenching constant.

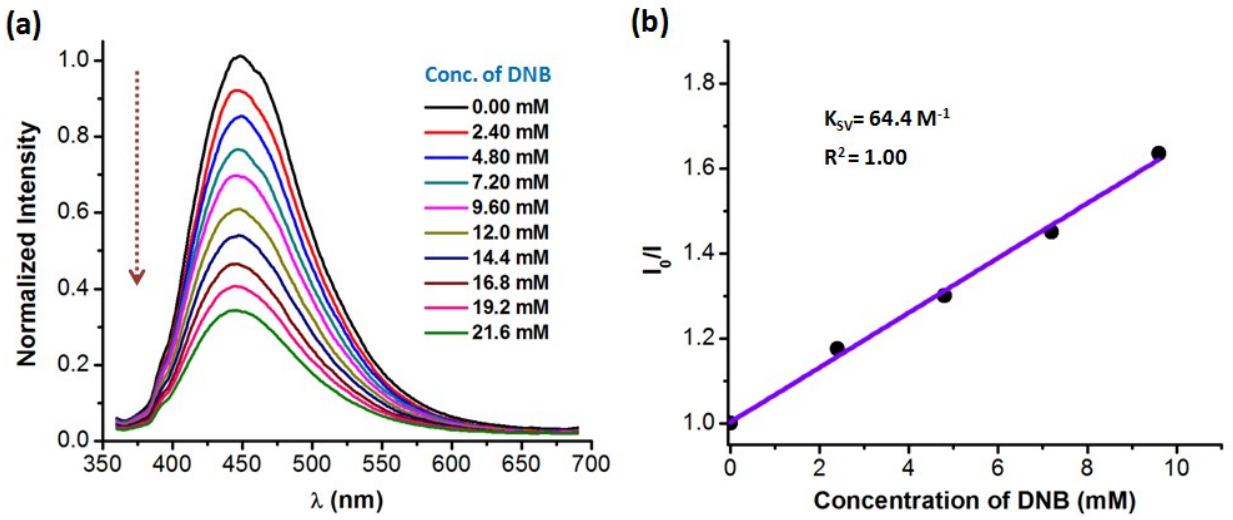

Fig. S23 (a) Quenching of fluorescence intensity of **H_6TPA** with increasing concentration of DNB in ethanol (λ_{ex} = 350 nm). (b) Determination of the Stern-Volmer quenching constant.

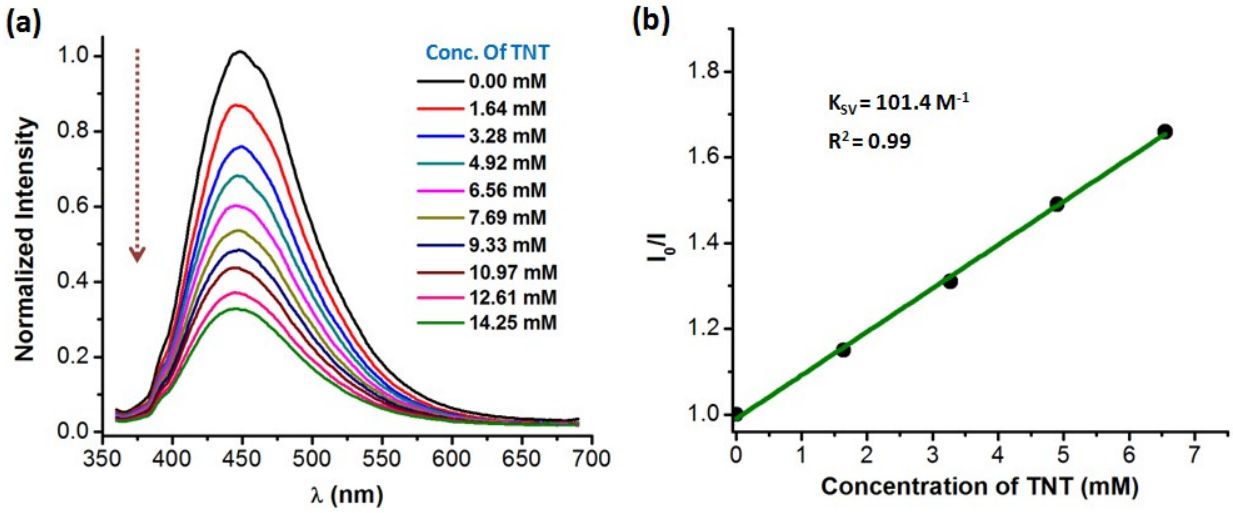

Fig. S24 (a) Quenching of fluorescence intensity of **H_6TPA** with increasing concentration of TNT in ethanol (λ_{ex} = 350 nm). (b) Determination of the Stern-Volmer quenching constant.

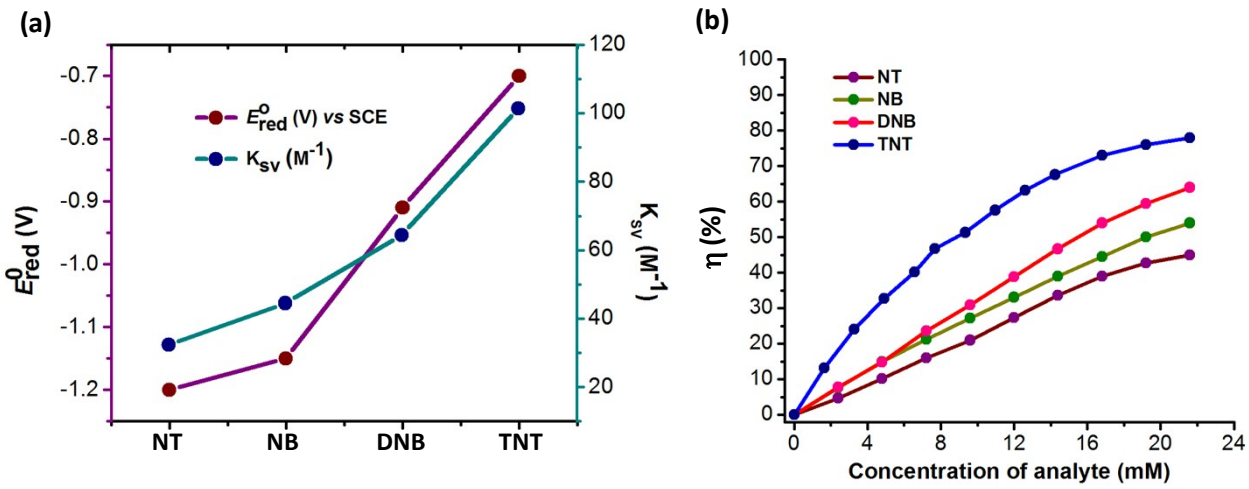

Fig. S25 (a) The correlation between reduction potentials and Stern–Volmer quenching constants of various nitroaromatic analytes (b) A plot of quenching efficiency versus concentration for each of the nitroaromatic analytes for **H_6TPA.**

Table S2. Reduction potentials and **H_6TPA** fluorescence quenching data for various NACs.

NAC	E^0_{red} (V vs. SCE)	K_{SV} (M^{-1})
NT	-1.20	32.3
NB	-1.15	44.5
DNB	-0.91	64.4
TNT	-0.70	101.4

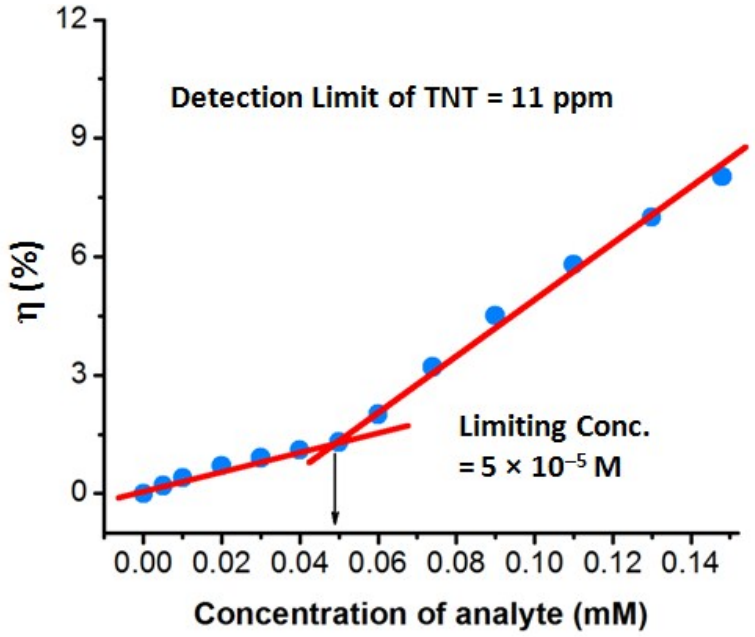

Fig. S26 Determination of the sensitivity of **In-TPA** towards the detection of TNT. Notice that the limiting concentration has been calculated from the point of intersection of the two linear fits that are colored in red. The ppm (i.e., mg/L) values are calculated as follows x (in ppm) = y (limiting conc. M) x MW/1000.

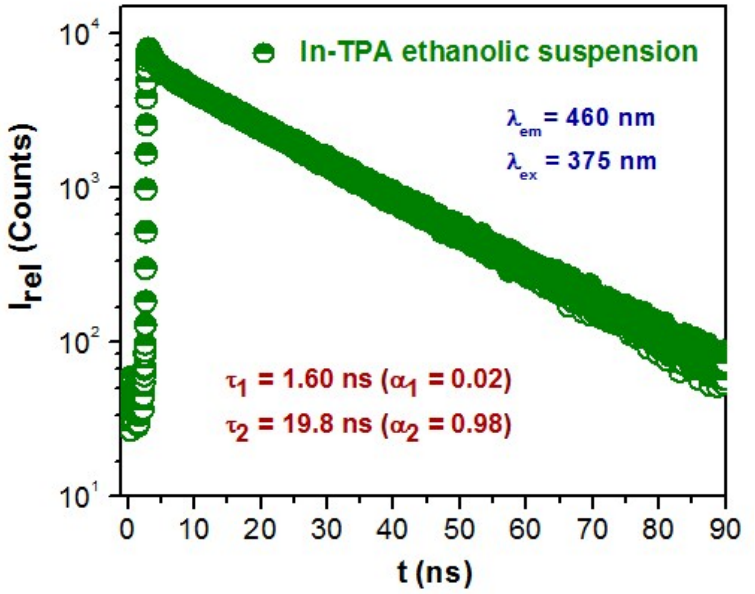

Fig. S27 Fluorescence lifetime decay trace (λ_{ex} = 375 nm; λ_{em} = 460 nm) of the ethanolic suspension of **In-TPA**.

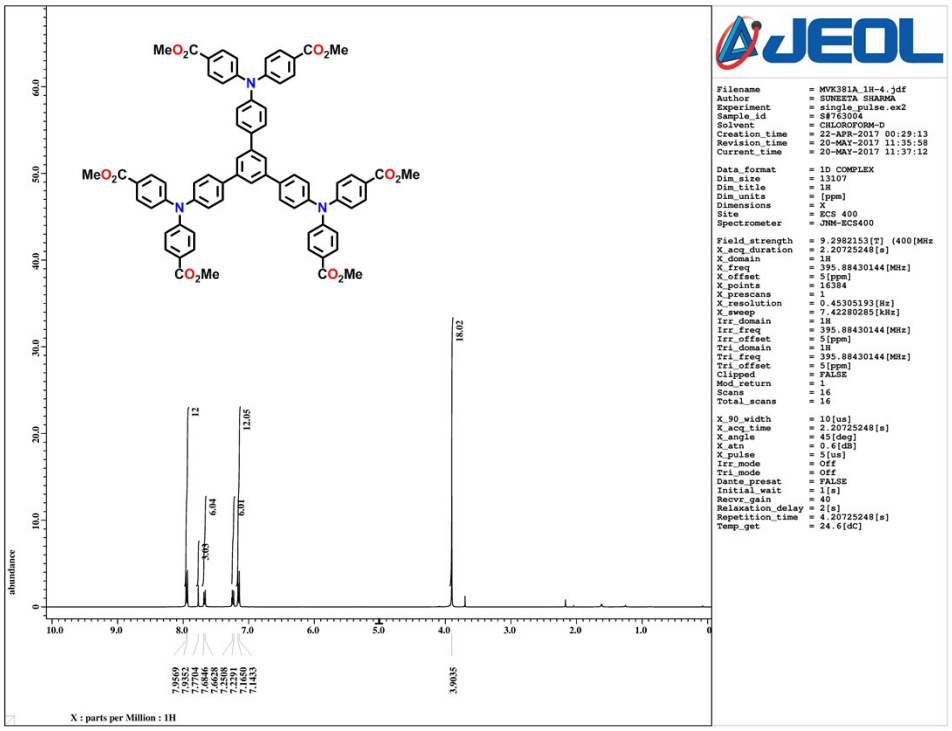

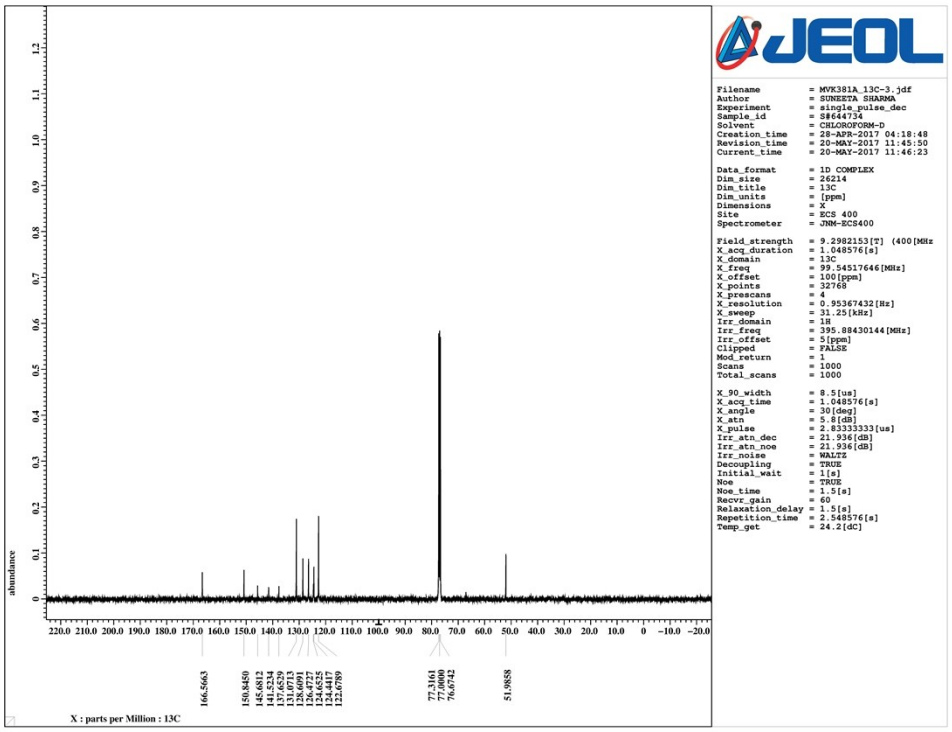

Fig. S28 ^{1}H NMR (400 MHz, $CDCl_3$) and ^{13}C NMR (100 MHz, $CDCl_3$) spectra of **2**.

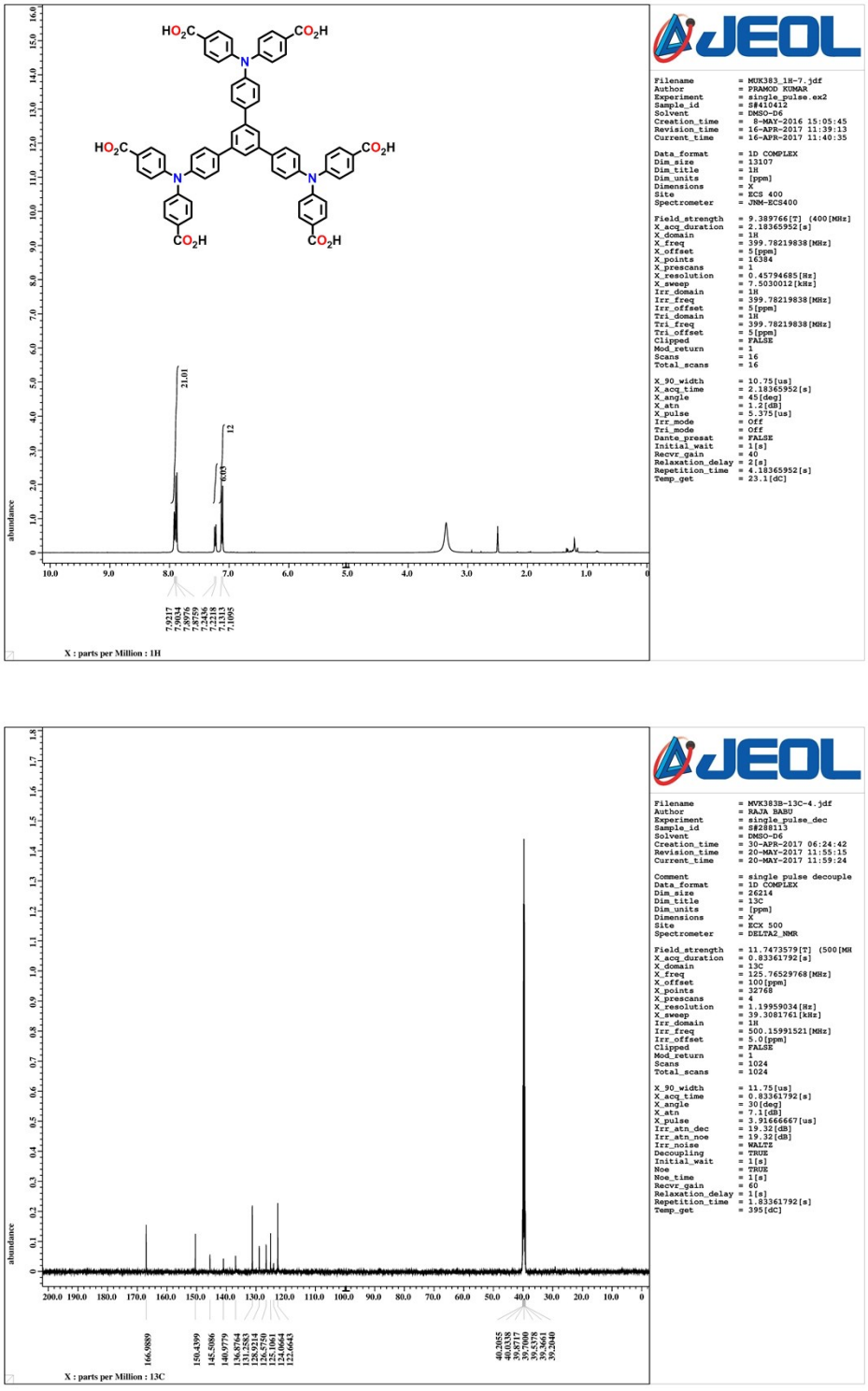

Fig. S29 ^{1}H NMR (400 MHz, DMSO-d_6) and ^{13}C NMR (125 MHz, DMSO-d_6) spectra of **H_6TPA**.